Eur. Phys. J. A **13**, 197–202 (2002)

THE EUROPEAN PHYSICAL JOURNAL A

Challenge towards muonic atom formation with unstable nuclei

P. Strasser[1], T. Matsuzaki[1], and K. Nagamine[1,2]

[1] Muon Science Laboratory, Institute of Physical and Chemical Research (RIKEN), 2-1 Hirosawa, Wako-shi, Saitama 351-0198, Japan

[2] Meson Science Laboratory, Institute of Materials Structure Science, High Energy Accelerator Research Organization (KEK), 1-1 Oho, Tsukuba-shi, Ibaraki 305-0801, Japan

Received: 1 May 2001

Abstract. X-ray spectroscopy of muonic atoms is an important tool to obtain information on the nuclear charge distribution of nuclei. It has been successfully used for many years to study stable isotopes in condensed or gaseous states. A new method has been proposed to extend muonic atom X-ray spectroscopy to the use of radioactive isotope beams to form muonic atoms with unstable nuclei. This new method allows studies of the nuclear properties and nuclear sizes of unstable atoms by means of the muonic X-ray method at facilities where both negative muon and radioactive nuclear beams would be available. Progress of a feasibility study at RIKEN-RAL muon facility is also reported.

PACS. 36.10.Dr Positronium, muonium, muonic atoms and molecules – 29.30.Kv X- and gamma-ray spectroscopy – 61.72.Ww Doping and impurity implantation in other materials

1 Introduction

The determination of nuclear properties and nuclear sizes using the tool of muonic atom spectroscopy has already a long history [1,2]. It has been successfully used for many years to study stable isotopes in condensed or gaseous states. Recently we proposed a new method [3] to extend X-ray spectroscopy of muonic atoms to the use of nuclear beams, including in the future radioactive isotope beams, which would allow studies of short-lived isotopes by means of the muonic X-ray method. When muonic X-ray spectroscopy with unstable nuclei becomes feasible, a new dimension in the study of nuclear physics will be opened. This would increase our knowledge of the nuclear structure far from the valley of stability, in particular the nuclear charge distribution and the deformation properties of nuclei.

X-ray transition energies in muonic atoms are strongly affected by the size of nuclei, and can be used efficiently to determine the nuclear charge distribution [1,2,4]. This usefully complements the knowledge obtained from electron scattering (stable isotopes), as the uncertainties of the absolute value of the root mean square (rms) radius are generally smaller when measured with muonic atoms [5]. Before comparing theoretical muonic transition energies for a given charge density with experiments, some well-defined theoretical corrections must be applied, namely the quantum electrodynamic corrections like the vacuum polarization and the Lamb shift, the nuclear polarization corrections, and the electron screening corrections [2,6]. The overall accuracy is presently limited by the nuclear polarization calculations having the largest uncertainty of all corrections, and being large compared to the present experimental accuracy achieved with high-resolution semiconductor detectors. The determination of these nuclear polarization effects are still a challenge to both theoreticians and experimentalists [6]. This makes, for the moment at least, the competition with the measurement of optical isotope shifts of short-lived isotopes by collinear laser spectroscopy (see, *e.g.*, ref. [7]) difficult. It should be noted, however, that a muonic isotope shift can be measured with accuracies slightly higher than those achieved for absolute muonic transition energies, because of relatively smaller uncertainties in the nuclear polarization corrections.

In addition, measurements of the quadrupole hyperfine splittings of muonic X-rays can also yield precise and reliable absolute values of nuclear quadrupole moments, which are sensitive to the deviation of the shape of a nuclear charge distribution from spherical symmetry.

2 Towards muonic atom spectroscopy with unstable nuclei

To combine a negative muon (μ^-) beam with a radioactive ion (Z^+) beam, and allow unstable muonic $Z(\mu Z)$ atoms to be formed, a common stopping medium is required. The idea that was proposed [3] is to use a thin solid hydrogen film where both μ^- and Z^+ are stopped simultaneously,

followed by the direct muon transfer reaction to higher-Z nuclei to form μZ muonic atoms.

2.1 Muonic atom formation with unstable nuclei

Figure 1 shows the proposed scheme of muonic atom formation with implanted ions in a solid hydrogen film using the two-layer arrangement [8,9]. The first layer —consisting of a hydrogen-deuterium (H_2/D_2) mixture (1 mm thick with a D_2 concentration of 0.001)— is used for μ^- stopping, followed by muonic protium ($p\mu$) atom formation, muon transfer to form muonic deuterium ($d\mu$) atoms, and $d\mu$ diffusion with the help of the Ramsauer-Townsend effect in the scattering of $d\mu$ atoms. The second layer —pure deuterium (D_2) with implanted Z^+ ions as impurities— is used for the formation of μZ atoms. Experimental results showed that a sizable fraction of incident μ^- (as high as 0.01, depending on the incoming μ^- beam momentum spread) are released as $\sim$ eV $d\mu$ atoms from the first H_2/D_2 layer surface [10]. Also, it was found that those energetic $d\mu$ atoms are stopped within a thickness of 5 μm of the added D_2 layer [9]. Consequently, if impurity ions are implanted into this D_2 layer, muon transfer from $d\mu$ atoms to higher Z nuclei will occur.

It is well known that when hydrogen is enriched in elements with atomic number $Z > 1$, the transfer of a muon from hydrogen to nuclei of heavy elements will inexorably take place [11], *i.e.*, $H\mu + Z \rightarrow \mu Z +$ H, with H $\equiv$ p, d. This direct transfer reaction is irreversible since the increase in binding energy greatly exceeds any attainable target temperature. It proceeds mainly to highly excited levels of the muonic atom μZ, being accompanied

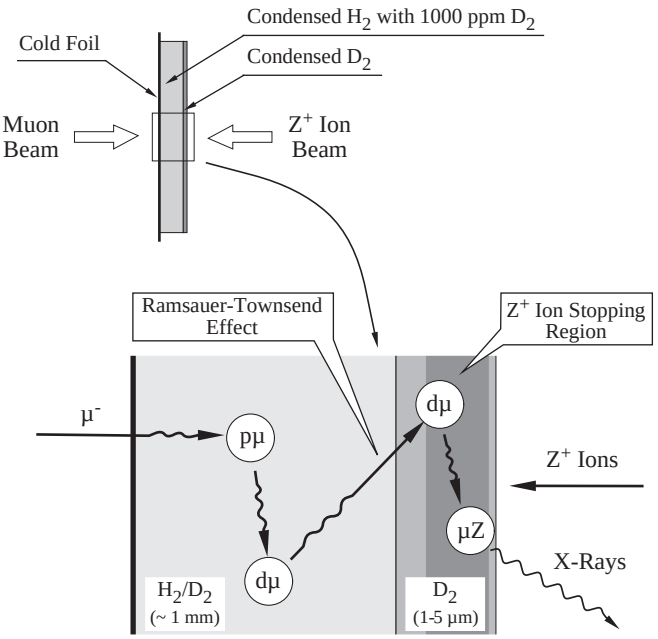

Fig. 1. Simplified scheme of muonic atom formation from implanted ions in solid hydrogen films using the two-layer arrangement.

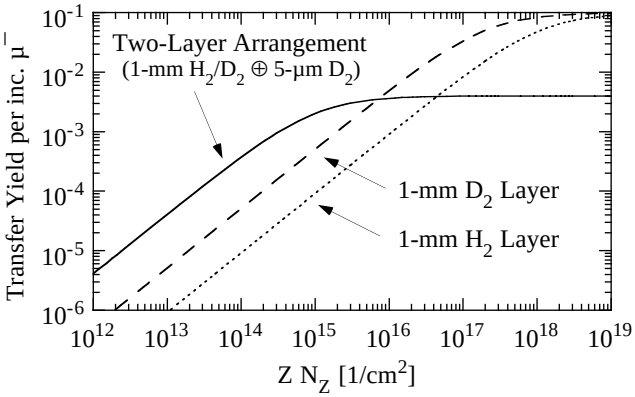

Fig. 2. Estimated transfer yield to implanted ions uniformly stopped in a 5 μm D_2 layer (two-layer arrangement case) (solid line). For comparison, the transfer yields obtained with the same ion number uniformly implanted in 1 mm H_2 (dotted line) and 1 mm D_2 (dashed line) layers are also shown.

by emission of characteristic X-rays and Auger electrons in the de-excitation of the μZ muonic atom. The transfer rate of this process in liquid-hydrogen is very fast (except for transitions to helium) and, as a rule, can be expressed as $\lambda_Z \approx ZC_Z \times 10^{10}\mathrm{s}^{-1}$ [11], where Z is the atomic number and C_Z is the concentration of higher-Z nuclei (*i.e.*, $C_Z = N_Z/N_\mathrm{X}$, with X $\equiv$ H, D). It should be noted, however, that the idea which makes use of the transfer mechanism is not new. It was already used 30 years ago to measure transfer rates and rms radii of rare isotopes with high-pressure gas target (see, *e.g.*, ref. [12]). The main advantage of using a solid hydrogen film for implantation of unstable nuclei is that it can be easily evaporated and replaced by a new one when the accumulation of daughter nuclei becomes significant. Moreover, by using the two-layer arrangement, the production region of the μZ atoms is confined to an optimized film thickness, resulting in a requirement on the beam energy for ion implantation much less severe for a thinner layer. For instance, to obtain a range of 1 mm in solid hydrogen, the ion energy required is already several tens of MeV/amu, while for 5 μm it is around 40 keV/amu.

2.2 Transfer yield estimation

In the two-layer arrangement case, the total transfer yield to implanted ions in the D_2 layer can be approximated as follows (neglecting muon sticking after $dd\mu$ fusion):

$$Y_Z = \frac{\phi\lambda_Z}{\lambda_0 + \phi\lambda_Z} Y_\mu Y_{\mathrm{d}\mu}, \qquad (1)$$

where λ_0 is the muon decay rate, ϕ is the number density of the D_2 layer (normalized to liquid-hydrogen density), Y_μ is the μ^- stopping yield in 1 mm H_2/D_2, and $Y_{\mathrm{d}\mu}$ is the fraction of stopped μ^- entering the D_2 layer as $d\mu$ atoms. In a previous experiment, we obtained the values of $Y_\mu \cong 0.1$ and $Y_{\mathrm{d}\mu} \cong 0.04$, respectively [9].

Figure 2 shows the estimated transfer yield as a function of ZN_Z (the atomic number Z multiplied by the

implanted ion number N_Z) for the two-layer arrangement assuming a uniform stopping region of implanted ions in the 5 μm D_2 layer (solid line). We also supposed that all emitted dμ atoms are stopped in this 5 μm D_2 layer (no dμ loss). For comparison, the transfer yields obtained with the same ion number implanted uniformly in 1 mm thick pure H_2 (dotted line) and pure D_2 (dashed line) layers, respectively, are also shown, using the same μ^- stopping yield Y_μ. Almost one order of magnitude higher transfer yield is achieved using the two-layer arrangement compared to a pure D_2 layer. In the case of a pure H_2 layer, the yield becomes even smaller because of the losses due to ppμ muonic molecule formation.

As an example, let us consider a target of 1 cm^2 with an incident muon beam intensity (N_μ) at 30 MeV/c of 10^8 μ^- per second (21st century muon beam facility [13] and under a superconducting Helmholtz coil confinement field), and $N_Z = 10^{12}$ implanted Sn ions ($Z = 50$). Then, we could expect $\sim 2 \times 10^4$ muonic tin (μSn) atoms to be formed per second, and $\sim$ 500 μSn $2p \rightarrow 1s$ transition photons (3.4 MeV) to be detected per hour, assuming an X-ray detection efficiency of 0.005, a detector solid angle of 0.002 and a branching ratio of 0.7. The main uncertainty in this preliminary yield estimation is the dμ loss from the D_2 layer that was neglected. It is expected to reduce the transfer yield for low ion concentration C_Z. Furthermore, solid state effects that appear in the dμ thermalization in solid hydrogen [14] may also affect directly this loss.

To improve the overall efficiency, one way would be to confine the emitted dμ atoms to a thinner D_2 layer thickness, reducing the implantation thickness and therefore the ion number required. In principle, this could be done by using thin lithium layers, as it was first proposed by Taqqu to improve the efficiency for slow μ^- production using a similar solid hydrogen target [15]. The idea was that thin lithium layers are quasi transparent to eV dμ atoms but highly reflective at low energy (below 0.1 eV). Another possibility would be to make use of the solid state effects that appear in low energy pμ atom scattering in solid H_2 [16]. At very low pμ energies ($\lesssim$ 2 meV), the total scattering cross-section falls by several orders of magnitude, the H_2 layer becomes transparent and a sizable fraction of pμ atoms is being emitted from the H_2 layer as cold pμ atoms, similarly to dμ atoms with the Ramsauer-Townsend effect. Then, if impurity ions are implanted near the H_2 surface, transfer from cold pμ atoms to higher Z nuclei may efficiently occur. More detailed investigations are required to examine these new schemes. Monte Carlo simulations are in progress to take into account all these effects, and optimize the total transfer yield.

2.3 Implantation of unstable nuclei

Several practical considerations in accomplishing the proposed experiment were already briefly mentioned in ref. [3]. One that needs particular attention is the accumulation of daughter nuclei in the target, because this gives a practical limitation to the shortest-lived isotopes that can be studied using this method.

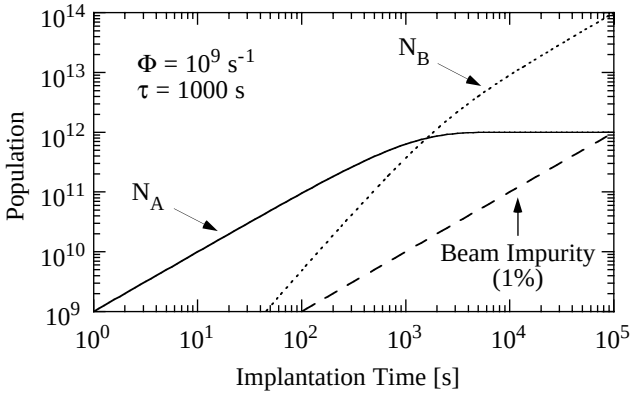

Fig. 3. Time dependence of implanted unstable nuclei (N_A, solid line) and daughter nuclei (N_B, dotted line) in the solid hydrogen target, considering a decay rate τ of 1000 s and a beam intensity Φ of 10^9 particles per second. The accumulation of a beam impurity of 1% is also shown (dashed line).

In this experiment, the radioactive isotope beam will be stopped completely in the solid hydrogen target. This is quite the opposite compared to nuclear astrophysics experiments that are planned with radioactive beams, where the beam only interacts with the target without actually stopping inside (only a small faction will be scattered and stopped inside the vacuum chamber vessel). The decay product, or daughter nuclei, will act as impurities in the hydrogen target and affect the total transfer yield to implanted unstable nuclei. The transfer rates being quite similar, the ratio between both populations will be the critical parameter. It should be noted that the limitation comes from the transfer yield that will be decreasing with time, and not from the X-ray measurement itself, since muonic transition energies of unstable nuclei and daughter nuclei are quite distinct (because of different atomic number) and can be easily distinguished using standard high-resolution semiconductor detectors.

As soon as the implantation of unstable nuclei starts with a beam intensity Φ, the number of unstable nuclei (N_A) and daughter nuclei (N_B) in the hydrogen target will increase. Both populations will be the same at around 1.6 times the decay time τ, and when the steady state is reached, N_A will saturate at a value of $\Phi\tau$ ($= N_Z$), while N_B will continue to increase with time, *i.e.*, Φt. The ratio between unstable nuclei and daughter nuclei (N_A/N_B) will be decreasing as $\tau/(t-\tau)$. At five times the decay time, this ratio will be nearly 0.25. As an example, fig. 3 shows the time dependence of each population, considering a decay rate τ of 1000 s ($T_{1/2} = 11$ min) and a beam intensity Φ of 10^9 particles per second. The effect of a beam impurity of 1% is also shown. We can notice that even if a small amount of contaminants is contained in the primary beam, the effect of the accumulation of daughter nuclei in the target is much more significant. Therefore, high-purity radioactive isotope beams are not essential to this experiment.

If a standard target system is used, after a certain period, the used hydrogen target will need to be evaporated

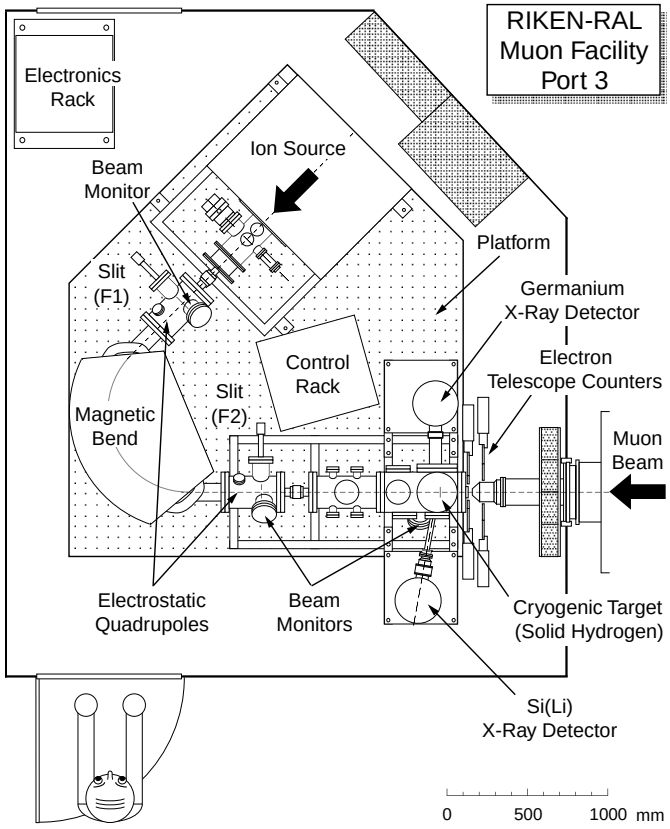

Fig. 4. Layout of the experimental setup for muonic atom X-ray spectroscopy with implanted ions in solid hydrogen films installed at RIKEN-RAL muon facility port 3.

and replaced by a new one. A few hours are needed at the moment to perform this operation. Therefore, we are practically limited with this method to study unstable nuclei with a half-life of a few tens of minutes, or longer. We could in principle use a rotating target, where the implantation region is changing with time, so that the area contaminated with daughter nuclei is regularly pushed away from the μ^- beam spot. This method could help to gain a factor of roughly ten, and allow unstable nuclei with a half-life of a few minutes to be studied.

The activity deposited by the radioactive isotope beam in the solid hydrogen target will also need to be carefully considered. It will reach a maximum value at the steady state equal to the beam intensity Φ. This will result in high radiation background making the measurement of muonic X-rays difficult. Without any doubt, the use a pulsed muon beam will help to reduce this background noise by several orders of magnitude [17]. The detection system will have to be designed specifically depending on the decay mode of the unstable nuclei to be studied to further minimize this background (*e.g.*, detector segmentation, active background suppression).

3 Test experiment

An experimental setup has been constructed to implant stable ions in solid hydrogen films using a cryogenic target combined with an ion implantation system. The objective is to establish experimentally the feasibility of this method, and determine the optimum conditions to perform muonic atom X-ray spectroscopy with implanted ions. Figure 4 shows the layout of this experimental setup installed at RIKEN-RAL muon facility port 3. The design and construction was already reported in detail in ref. [18]. In brief, it comprises mainly two parts: 1) a cryogenic target system to cool a silver foil down to 3 K onto which a thin target layer of solid hydrogen is formed by freezing the hydrogen gas using a diffuser, and 2) an ion source with an analyzing magnet to accelerate, select and implant stable ions into this solid hydrogen film. All the components of this setup were mounted on a platform 700 mm high for quick installation and removal from the experimental area, this one being used by many other users.

The cryogenic target system is mainly constituted of a helium cryostat used to cool down a 100 μm thick silver foil (cold foil) to around 3 K. It was designed to sustain the additional power load deposited by the ion beam, ensuring a temperature at the center of the target below 4 K (*e.g.*, a 10 μA 50 keV ion beam would deposit 0.5 W on the target). Moreover, the key feature of this cryogenic target system is the liquid-helium (LHe) reservoir of the cryostat being at atmospheric pressure, so that it can be refilled without any disturbance to the good operation of the system. This allows a solid hydrogen target to be kept indefinitely as long as the LHe reservoir is refilled on a regular basis (typically once a day). The same technique as employed in previous experiments [19,8,9] is used to deposit hydrogen films. A thin target layer of solid hydrogen is formed by freezing the hydrogen gas (H_2 and/or D_2) onto the cold foil held at 3 K. The hydrogen is deposited with a removable diffuser —a stainless-steel foil perforated with holes located 10 mm away from the cold foil. A known pressure of hydrogen gas at a standard volume is allowed to escape slowly through the diffuser and impinge upon the cold Ag foil. Before the measurement, the diffuser is removed.

Impurity ions are then implanted in the surface of the film using a dedicated ion source with an electrostatic accelerator and a transportation optics. The ions are produced with a duoplasmatron ion source (mainly from noble gases), accelerated by a strong electric field up to an energy of 33 keV/q, and focussed using a double stage Einzel lens to the first focal point (F1) (see fig. 4). Then, they are mass and charge analyzed using a magnetic sector with 135 degree deflection. This system is stigmatically point-to-point focusing from F1 to F2. Two electrostatic quadrupoles are used, before and after, to compensate the fringing field of the magnet. At F2, the ions are selected with a horizontal slit, before being directed to the target to be implanted within a diameter of 30–40 mm to match the size of the negative muon beam. Three beam profile monitors are used to determine the ion beam profile and current. They are located after the two slits (F1 and F2) and about 10 cm before the solid hydrogen target, respectively. The implantation depth is tuned by changing the acceleration voltage of the ion source, and alternate

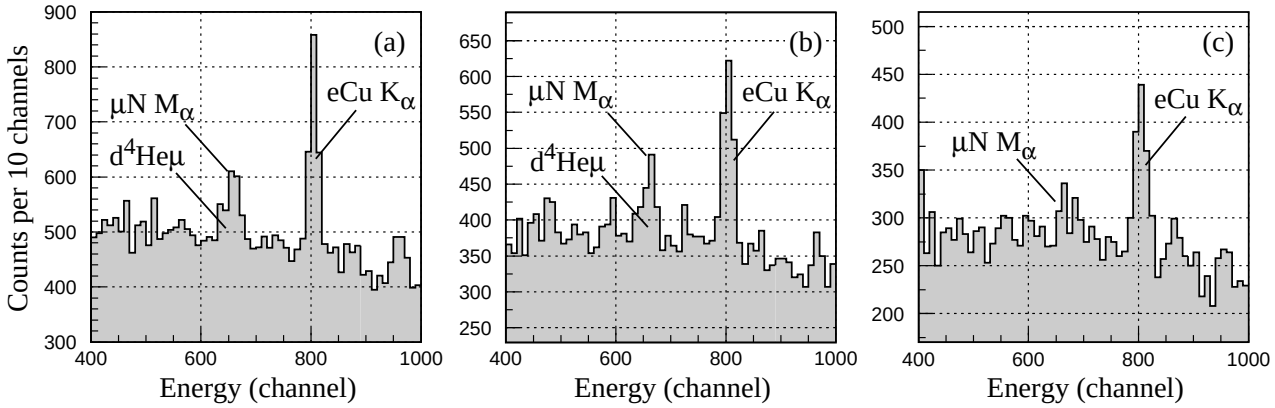

Fig. 5. Si(Li) detector total X-ray energy spectra measured with the two-layer arrangement and (a) 100 ppm, (b) 200 ppm and (c) without ^{4}He ions implanted in a 5 μm D_2 layer thickness (preliminary data). One channel corresponds to $\sim$ 10 eV.

hydrogen deposition and ion implantation can be used to obtain a larger implantation depth. The total number of ions implanted in the film is determined by the ion beam current at the target and the implantation time, while the ion distribution profile in the film is calculated using the the Monte Carlo code SRIM 2000 [20].

A Si(Li) detector and a germanium X-ray detector are used to detect muonic X-rays emitted from muonic atoms. The key feature is the head of the Si(Li) detector (70 mm^2 and 5 mm thick, with a 25 μm Be window) located inside the target chamber, which directly faces the solid hydrogen target to allow very low-energy X-rays such as pμ K_α (1.9 keV) to be detected at a high transmission efficiency [19,8,9]. The germanium X-ray detector, placed outside the target chamber behind a 100 μm stainless-steel window and a 10 μm silver window (cryostat shield), is used to detect higher-energy X-rays. Two telescope scintillation counters, also placed outside the target chamber, are used to detect decay e^- from muons to determine the number of stopped μ^- in the target.

It should be noted that muonic processes in hydrogen are very sensitive to any contamination from heavier nuclei due to transfer reactions which compete strongly with the reactions being investigated. Therefore, cleanliness and a high-vacuum environment should be ensured in the target chamber. Since this requirement is not compatible with the normal operation of an ion source, a differential pumping system is used to separate the poor vacuum of the ion source from that of the target chamber. In addition, hydrogen gas purification is also required before target preparation.

4 First experimental results

A first test experiment was conducted at RIKEN-RAL muon facility port 3 in September 2000. The overall operation of the experimental setup was found to be satisfactory as designed. The setup was used to implant helium (^{4}He) ions in a solid deuterium film to study muon transfer reactions from deuterium to helium in solid.

This process is crucial in muon catalyzed fusion (μCF) with deuterium and tritium (DT) mixtures, since helium is accumulated in the target due to tritium beta-decay (^{3}He), and nuclear fusion reactions (^{4}He). While X-ray studies have already been carried out in liquid hydrogen and deuterium with helium admixtures by pressurizing the liquid surface with helium gas [21,22], the present technique allows the study of this process in solid. Moreover, in recent μCF experiments at RIKEN-RAL Muon Facility, an effect due to the ^{3}He accumulation in solid was discovered [23]. ^{3}He produced in solid DT mixtures is trapped, while in liquid it diffuses out of the target. It was also found that when the ^{3}He concentration reaches about 130 ppm, there is a saturation effect showing a possible nucleation of ^{3}He, *i.e.*, several helium atoms gathering to make a cluster.

It should be emphasized that, in the case of helium, the muon transfer process from muonic hydrogen atoms to helium nuclei occurs predominantly through the formation of muonic molecules (*i.e.*, pHeμ, dHeμ or tHeμ). Photons are emitted from the radiative transition from the excited state of the muonic molecule to the unbound ground state with a central energy and width of 6.8 keV and 0.8 keV, respectively, and an asymmetric line shape showing a low-energy tail.

6.8 keV X-rays from the radiative decay of d^{4}Heμ molecules during the μ^- transfer process from dμ atoms to ^{4}He nuclei were successfully observed with the Si(Li) X-ray detector for the first time in solid deuterium. Figure 5 shows the preliminary data obtained with the two-layer arrangement and with, respectively, 100 ppm, 200 ppm and without ^{4}He ions implanted. Unfortunately, we suffered from a nitrogen contamination in our D_2 target which resulted in a severe competition for the muon transfer reaction to ^{4}He, and thus reducing considerably the expected X-ray yield. Moreover, muonic nitrogen (μN) M_α X-rays come just at 6.66 keV, more sharply than the 6.8 keV peak, but still disturbing considerably the measurement. The palladium filter, which was planned to be used during the experiment to purify the deuterium gas before depositing the target, was unfortunately out of order. It should

be noted, however, that muonic nitrogen peaks (*i.e.*, μN $L_{\alpha,\beta}$ and M_α) can only be distinguished when a thin D_2 layer is added to the primary H_2/D_2 layer with or without ^{4}He ions implanted. With 100 ppm ^{4}He, only about one third of the expected yield could be observed, and for 200 ppm even less. It is still too early to draw any conclusion, but this might reflect the saturation effect being investigated. The data are now being analyzed, and the results will be reported elsewhere in a later publication.

5 Future plans

Further experiments are being planned to implant stable ions (*e.g.*, Ar, Kr, Xe) in solid deuterium films, to establish experimentally the feasibility of this method and determine the optimum conditions to conduct muonic X-ray spectroscopy with implanted ions. Muon X-ray transitions energies and possibly muonic isotope shifts will be measured to determine nuclear charge radii.

More measurements of muon transfer reactions from deuterium to helium in solid, as a function of the helium concentration, are also in progress.

Finally, as an intermediate step towards muonic X-ray spectroscopy with unstable nuclei, an experiment using long-lived isotopes is also under consideration. An element selective ion source is now under development by Miyatake *et al.* [24]. One candidate element is ^{56}Ni (neutron and proton magic, $T_{1/2} = 6.1$ d). Other interesting elements considered include ^{146}Gd (neutron magic, $T_{1/2} = 48.3$ d), ^{148}Gd (systematics, $T_{1/2} = 74.6$ y), and ^{126}Sn (proton magic, $T_{1/2} = 10^5$ y).

6 Summary

This new method, which extends muonic atom X-ray spectroscopy to the use of nuclear beams, allows studies of the nuclear charge distribution and the deformation properties of unstable atoms by means of the muonic X-ray method at facilities where both negative muon and radioactive isotope beams would be available. Indeed, new radioactive nuclear beam projects are coming into operation (or being planned) at facilities where negative muon beams are also available, *e.g.*, the ISAC project at TRIUMF [25], the SIRIUS project at ISIS/RAL [26], the E-arena in the KEK-JAERI joint project (second phase) [27], and maybe the RI Beam Factory project at RIKEN [28], provided intense negative muon beams can be produced there.

In the longer term, we may hope that theoretical muonic transition energies may be calculated more accurately (in particular the nuclear polarization corrections) leading to higher precision in the determination of nuclear charge radii from the measurements of muonic atoms. Also, the properties of new cryogenic microcalorimeter X-ray and γ-ray detectors may have a potential of much higher energy resolution than that of existing germanium detectors (but with the disadvantage of lack of timing information).

One of the authors (PS) is grateful to Dr. K. Ishida for his help and collaboration during the test experiments performed at RIKEN-RAL, and to Drs. S.N. Nakamura and N. Kawamura for their support using the data acquisition EXP2K. Beneficial discussions with Dr. M. Wada and encouragement from Dr. R. Scheuermann are also acknowledged. Gratitude is extended to Drs. I. Watanabe, Y. Matsuda, K. Shimomura, A. Fukaya, K. Hashi, and Mr. P. Demarest for their helpful contributions during the construction of the experimental setup.

References

1. J. Hüfner, F. Scheck, C.S. Wu, in *Muon Physics*, edited by V.W. Hughes, C.S. Wu, Vol. **1** (Academic Press, New York, 1975) pp. 201–307.
2. R. Engfer *et al.*, At. Data Nucl. Data Tables **14**, 509 (1974).
3. P. Strasser *et al.*, Hyperfine Interact. **119**, 317 (1999).
4. L.A. Schaller, Z. Phys. C **56**, S48 (1992).
5. G. Fricke *et al.*, Phys. Rev. C **45**, 80 (1992).
6. E. Borie, G.A. Rinker, Rev. Mod. Phys. **54**, 67 (1982).
7. A.C. Mueller *et al.*, Nucl. Phys. A **403**, 234 (1983).
8. P. Strasser *et al.*, Phys. Lett. B **368**, 32 (1996).
9. P. Strasser *et al.*, Hyperfine Interact. **101/102**, 539 (1996).
10. B.M. Forster *et al.*, Hyperfine Interact. **65**, 1007 (1990).
11. S.S. Gershtein, L.I. Ponomarev, in *Muon Physics*, edited by V.W. Hughes, C.S. Wu, Vol. **3** (Academic Press, New York, 1975) pp. 151, 163–165, 190–194.
12. G. Backenstoss *et al.*, Phys. Lett. B **36**, 422 (1971).
13. K. Ishida *et al.*, in *Proceedings of the Workshop on Ultra-high Intensity Muon Beam and Muon Science in the 21st Century*, edited by S. Sakamoto, KEK Proceedings 99–11 (High Energy Accelerator Research Organization (KEK), 1999) p. 61.
14. A. Adamczak, Hyperfine Interact. **119**, 23 (1999).
15. D. Taqqu, Muon Catal. Fusion **5/6**, 543 (1990/91).
16. J. Woźniak *et al.*, Hyperfine Interact. **119**, 63 (1999).
17. K. Nagamine *et al.*, Muon Catal. Fusion **1**, 137 (1986).
18. P. Strasser *et al.*, Nucl. Instrum. Methods A **460**, 451 (2001).
19. P. Strasser *et al.*, Hyperfine Interact. **82**, 543 (1993).
20. J.F. Ziegler, J.P. Biersack, U. Littmark, in *The Stopping and Ranges of Ions in Matter*, edited by J.F. Ziegler, Vol. **1** (Pergamon Press, New York, 1985); for further information and download see also `http://www.SRIM.org/`.
21. T. Matsuzaki *et al.*, Muon Catal. Fusion **2**, 217 (1988).
22. K. Ishida *et al.*, Hyperfine Interact. **82**, 111 (1993).
23. N. Kawamura *et al.*, Phys. Lett. B **465**, 74 (1999).
24. H. Miyatake, private communication.
25. P. Bricault *et al.*, in *Proceedings of the 5th International Conference on Radioactive Nuclear Beams RBN2000, Divonne, France, April 2000*, to be published in Nucl. Phys. A.
26. In *SIRIUS Science* (1998) and *SIRIUS Technical Description* (1999) Booklets, Council for the Central Laboratory of the Research Councils; inquiries at The Librarian, Rutherford Appleton Laboratory, Chilton, Didcot, Oxfordshire OX11 0QX, UK.
27. H. Miyatake *et al.*, in *Proceedings of the 5th International Conference on Radioactive Nuclear Beams RBN2000, Divonne, France, April 2000*, to be published in Nucl. Phys. A.
28. I. Tanihata, Nucl. Phys. A **616**, 56c (1997).